Novel RFI Mitigation Methods in the Square Kilometre Array 1 Mid Correlator Beamformer

Thushara Gunaratne[1], Brent Carlson[1] and Gianni Comoretto[2].
[1]*Hertzberg Astronomy and Astrophysics Research Center, National Research Council Canada, Po Box 248, Penticton, British Columbia, CANADA, Thushara.Gunaratne@nrc-cnrc.gc.ca*
[2]Arcetri Astrophysical Observatory, *5 Largo Fermi, Firenze, ITALY, comore@arcetri.astro.it*

Received (to be inserted by publisher); Revised (to be inserted by publisher); Accepted (to be inserted by publisher);

The Square Kilometre Array (SKA) Phase 1 Mid Correlator Beamformer (CBF) adopts two novel methods to mitigate radio frequency interference (RFI) at the various stages of its signal chains. First, the pioneering Sample Clock Frequency Offset (SCFO) sampling suppresses interference which leaks into individual 'Frequency-Slice' (FS) (sub-bands) in the cross-correlations. Second, the 'Shift-Resample-Shift-Back' method minimizes the addition of noise due to strong clustered RFI. Empirical studies conducted with simulation of the systems confirm that the proposed methods significantly reduce the impact of RFI on the output of the radio telescope.

Keywords: Frequency-Slice, RFI, SCFO, SKA.

1. Introduction

The first phase of the Square Kilometre Array (SKA1) (www.skatelescope.org) includes the world's largest astronomical telescope operating in the "middle" radio frequency range (0.35-15.3 GHz). Built in the Karoo desert in South Africa, SKA1_Mid is expected to be 5 – 10 times more sensitive and have 10 times faster survey speed than the best existing instruments (SKAO/Info Sheet). The expected sensitivity and dynamic range lead to strict requirements on RFI mitigation (Dewdney, 2016).

The South African site was selected in large part for its low levels of RFI, and the South African government has legislated provisions to protect the site from future RFI contamination (Astronomy Geographic Advantage [AGA] Act). In June 2013, Independent Communications Authority of South Africa gazetted the allocated band for the SKA. However, despite these efforts, recent measurements (Mesa Solutions, 2018) have shown that significant levels of RFI exist at the site, with potentially severe implications for astronomical observations.

In order to mitigate the effects of such RFI, several strategies have been adopted along the entire signal chain of SKA1_Mid (Dewdney, 2016). In particular, the Mid Correlator and Beamformer (Mid.CBF) adopts two novel approaches to RFI mitigation, augmenting the conventional 'detect and flag' approach (Gunaratne et al., 2016). First, in the Sample Clock Frequency Offset (SCFO) sampling method (Carlson, 2016), each SKA1_Mid receptor is sampled at different samples rates, and as a result RFI leaking into different Frequency Slices (FSs) appears at different frequencies. Hence, when cross-correlated, the leaked RFI components decorrelate in proportion with the integration time and the frequency offset. Second, the 'Shift-Resample-Shift-Back' method reduces the effect of strong RFI with high time occupancy that is clustered in frequency (e.g. GSM, Digital-TV and GNSS). This method is facilitated by the Frequency Slice Architecture adopted by the Mid.CBF. Here, the FSs, which each process an ~200 MHz chunk of the observing band, are shifted to re-orient the strong RFI near the DC edge (i.e. 0 Hz). The FS then performs resampling to correct for SCFO sampling and delay-tracking and shift-back to return to the original frequency sense. Resampling with a 'fractional-delay filter-bank' with a finite number of delay-steps causes systematic sample-time jitters that create replicas of the input spectrum. These replicas can be suppressed by adding a random delay-jitter, but this increases the noise floor of the system. However, the added noise power is proportional to the absolute magnitude of the resampling error. By moving the strong RFI close to the DC edge, the absolute error due to resampling becomes low, and the system noise floor recedes.

2. SCFO Sampling for RFI Mitigation

2.1. *An Introduction to SCFO Sampling*

In the SKA1 Mid telescope, Sample Clock Frequency Offset (SCFO) sampling is used not only to mitigate out-of-Frequency Slice (FS) interference, but also to suppress digitizer-generated self-interference (Carlson, 2016). In SCFO sampling the received signals at each receptor are sampled at slightly different sample rates. Subsequently, these sampled sequences are digitally re-sampled to a common sample rate prior to correlation/beamforming.

As shown in (Carlson, 2016), out-of-FS interference features that alias into the passband are at different frequencies because the signals for different receptors are sampled at different sampling rates. Similarly, the spectral artefacts generated by the non-ideal sampling process (i.e., phase noise and non-uniform quantization levels, etc.) are at different frequencies due to the different sampling rates. It has been shown that for two complex-sinusoids $A_1 e^{j\omega_1 n}$ and $A_2 e^{j\omega_2 n}$, the cross-correlation for N-samples is given by

$$\langle A_1 e^{j\omega_1 n} \cdot \left(A_2 e^{j\omega_2 n}\right)^* \rangle_N = A_1 A_2 \mathrm{sinc}\left(\frac{(\omega_1 - \omega_2)N}{2}\right). \quad (1)$$

This implies that in noise-free channels the power level should go down inversely proportional to the frequency difference and the samples in the integration. However, if there is uncorrelated noise associated with the two channels such that $x_1(n) = A_1 e^{j\omega_1 n} + n_1(n)$ and $x_2(n) = A_2 e^{j\omega_2 n} + n_2(n)$, the cross-correlation for N-samples is given by

$$\begin{aligned} \langle x_1(n) \cdot x_1^*(n) \rangle_N = \quad & \langle A_1 e^{j\omega_1 n} \cdot \left(A_2 e^{j\omega_2 n}\right)^* \rangle_N + \langle n_1(n) \cdot \left(A_2 e^{j\omega_2 n}\right)^* \rangle_N \\ & + \langle A_1 e^{j\omega_1 n} \cdot \left(n_2(n)\right)^* \rangle_N + \langle n_1(n) \cdot n_2^*(n) \rangle_N, \end{aligned} \quad (2)$$

where $n_1(n)$ and $n_2(n)$ are Gaussian random variables of zero mean and variance σ_1^2 and σ_2^2, respectively. Following (1) and identities of Gaussian random variables (Woyczynski, 2010), (2) can be expressed as

$$\langle x_1(n) \cdot x_2^*(n) \rangle_N = A_1 A_2 \mathrm{sinc}\left(\tfrac{(\omega_1 - \omega_2)N}{2}\right) + A_2 \langle \acute{n}_1(n) \rangle_N + A_1 \langle \acute{n}_2(n) \rangle_N + \langle n_1(n) \cdot n_2^*(n) \rangle_N, \quad (3)$$

where $\acute{n}_1(n)$ and $\acute{n}_2(n)$ are frequency-shifted versions of $n_1(n)$ and $n_2(n)$, respectively. Hence, it can be shown that $\langle \acute{n}_1(n) \rangle_N$ and $\langle \acute{n}_1(n) \rangle_N$ are Gaussian random variables of zero mean and variance $\sigma_1^2/\sqrt{N}$ and $\sigma_2^2/\sqrt{N}$, respectively. Also it has been shown that $\langle n_1(n) \cdot n_2^*(n) \rangle_N$ is a random variable with zero mean and variance $(\sigma_1^2 \cdot \sigma_2^2)/\sqrt{N}$.

For a different implementation of the Mid.CBF, the performance of SCFO sampling has been studied empirically (Carlson & Gunaratne, 2017). In the following, the performance of SCFO sampling as proposed in the FSA for SKA1_Mid.CBF is studied with empirical simulations of end-to-end processing for the imaging/correlation signal chain in Mid.CBF.

2.2. *The Implementation of SCFO Sampling in Mid.CBF*

Adopting the FSA, the implementation of SCFO sampling in the SKA1 Mid telescope for the normal signal chain is shown in Fig. 1-(a). For sampling at the receptor (implemented by the DSH consortium), the different reference clocks $\{.., F_R(A_{n1}), .., F_R(A_{n2}), ..\}$ are synthesized by the Signal and Data Transport (SaDT) element of SKA1_Mid. In DSH, these synthesized reference clocks are used to generate band specific sampling clocks $\{.., F_S(A_{n1}), .., F_S(A_{n2}), ..\}$ by dividing/multiplying the reference clocks. For receptors $\{.., A_{n1}, .., A_{n2}, ..\}$, the sampled sequences $\{.., x[A_{n1}](n), .., x[A_{n2}](n), ..\}$ and the sample rates $\{.., F_S(A_{n1}), .., F_S(A_{n2}), ..\}$ are sent to the Mid.CBF. SaDT also sends the system 1 second marker (S-1PPS) and the reference clock F_{Mid} as the timing reference to the Mid.CBF for time stamping the visibilities.

For SKA1_Mid, the reference clock $F_R(A_n)$ (in Hz) for antenna A_n must be in the form

$$F_R(A_n) = 3.96 \times 10^9 + k(A_n) \cdot \Delta F, \tag{4}$$

where the 'offset-step' ΔF must be an integer multiple of 180 Hz and ΔF = 1.8 kHz is preferred. The 'offset index' $k(A_n)$ is a positive integer. Given that ΔF = 1.8 kHz, for a maximum net-offset of 4 MHz, $k(A_n) \in [1,2222]$. For each SKA1_Mid observing Band, the ratios used for generating sample clocks for the Analog to Digital Converters (ADCs) and the corresponding sampling rates are given in Table 1. Also, for SKA1_Mid Bands 4, 5a and 5b, DSH extracts 2.5 GHz of bandwidth from the sampled sequences using Digital Down Convertors (DDCs) at the sample rate of ~5.94 Gsps. The associated down sampling factors (DSFs) for the DDCs and the corresponding sample rates are listed in Table 1. Note that, when extracting SKA1_Mid Bands 5a and 5b, DSH applies *special frequency shift* $FS_{[a/b]}(A_n)$

$$\begin{aligned} \mathrm{FS}_{[\mathrm{a}]}(\mathrm{A_n}) &= 9/8(\mathrm{k}(\mathrm{A_n}) \cdot \Delta\mathrm{F} - 3617280), \\ \mathrm{FS}_{[\mathrm{b}]}(\mathrm{A_n}) &= 2(\mathrm{k}(\mathrm{A_n}) \cdot \Delta\mathrm{F} - 3617280), \end{aligned} \tag{5}$$

at the DDCs. This is to compensate for the excessive frequency shifts caused by Nyquist zone 2 SCFO sampling.

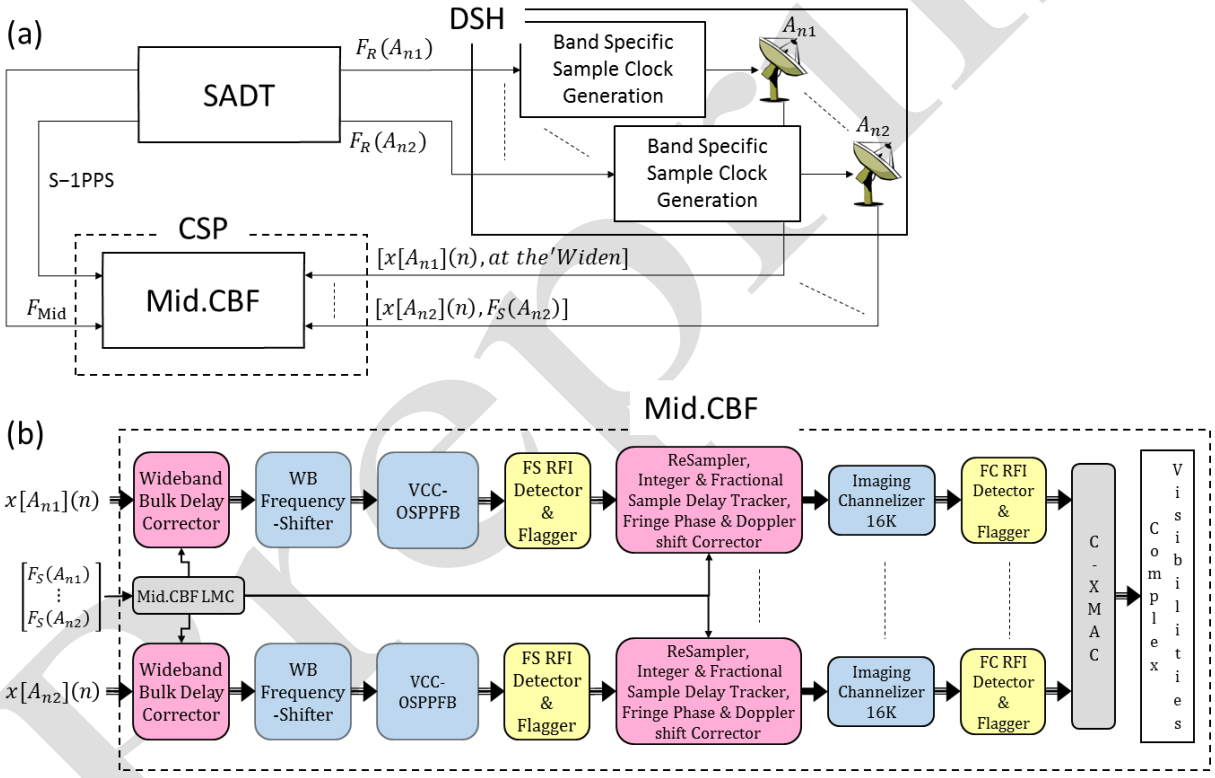

Fig. 1. An illustration of the implementation of the SCFO sampling in SKA Mid telescope.

At the Mid.CBF, which is illustrated with the signal processing modules for normal imaging in Fig. 1-(b), the input sequences $\{..,x[A_{n1}](n),..,x[A_{n2}](n),..\}$ are first corrected for the integer-sample delay in the 'Wideband Bulk Delay Corrector'. The bulk delay corrections are derived by the Local Monitor and Control (LMC) of the Mid.CBF considering the actual sampling rates and the delay correction modules provided by the SKA1 Telescope Manger (TM). For all Bands except Band 3, after the bulk delay correction, the wideband sample sequences are processed with the 'Wideband Frequency-Shifter' that reorients the wideband spectrum for subsequent extraction of the FSs with the Very Coarse Channelizer - Oversampled Polyphase Filter-Bank (VCC-OSPPFB). For Band 3, first, the bulk-delay-corrected sequences are up-sampled by the factor of $5/4$, allowing the Wideband Frequency-Shifter and VCC-OSPPFB used in Bands 1 and 2 to be used for Band 3 as well.

Table 1. The SKA1 Mid Bands, ADC sample clock to Reference clock ratios, actual sampling rates, DSF for the DSH DDC and sample rates delivered to the Mid.CBF.

SKA1 Mid Bands	ADC Clock to Ref: Clock Ratio	ADC Sampling Rate(Hz)	DDC DSF	Sample Rate to be Delivered to Mid.CBF (Hz)
3	1	$3.96 \times 10^9 + k(A_n)\Delta F$	1	$3.96 \times 10^9 + k(A_n)\Delta F$
2	1	$3.96 \times 10^9 + k(A_n)\Delta F$	1	$3.96 \times 10^9 + k(A_n)\Delta F$
3	4/5	$3.168 \times 10^9 + 4/5\ k(A_n)\Delta F$	1	$3.168 \times 10^9 + 4/5\ k(A_n)\Delta F$
4	4	$15.84 \times 10^9 + 4k(A_n)\Delta F$	8/3	$5.94 \times 10^9 + 3/2\ k(A_n)\Delta F$
5a	9/4	$8.91 \times 10^9 + 9/4\ k(A_n)\Delta F$	3/2	$5.94 \times 10^9 + 3/2\ k(A_n)\Delta F$
5b	4	$15.84 \times 10^9 + 4k(A_n)\Delta F$	8/3	$5.94 \times 10^9 + 3/2\ k(A_n)\Delta F$

At the output of VCC-OSPPFB, the FSs produced for different receptors are at different sample rates. Following the guidelines set by (Dewdney, 2016), immediately after the VCC-OSPPFBs, 'Frequency Slice (FS) RFI Detector & Flaggers' checks for RFI in each FS selected for subsequent processing and flags the corresponding data accordingly. The 'ReSampler' resamples the FS to a common sample rate of 220.20096 Msps and also corrects residual integer delays and fractional delays including phase offsets. The delay and phase corrections for the ReSampler are derived in the LMC of the Mid.CBF and sent in the form of 1st order polynomials. After resampling, the signal sequences are processed by the 'Imaging Channelizer', yielding 16,384 'critically-sampled' imaging fine channels. Each of these imaging fine channels is checked for RFI and flagged accordingly by the 'Fine Channel RFI Detector & Flaggers'. The fine channels are then processed by the 'Complex Cross-Multiplier Accumulator' (C-XMAC), which evaluates auto- and cross- correlations for all relevant receptor pairs. These auto- and cross-correlations are then time-stamped, packaged and sent to the SKA Science and Data Processor (SDP) for image formation.

Consider a strong RFI tone of frequency F_{RFI} with respect to the baseband spectrum of the sampled sequence. This RFI natively occurs in the N^{th} FS, where N is given by

$$N = \text{round}\left[\frac{N_{\text{FS}} \cdot F_{RFI}}{F_m}\right], \tag{6}$$

where F_m is the sample rate delivered to the Mid.CBF for the m^{th} receptor (see Table 1) and N_{FS} is the number of FS produced by the VCC-OSPPFB. Note that for Bands 1, 2 and 3, N_{FS} = 20, while for Bands 4, 5a and 5b, N_{FS} = 30. For any M^{th} FS, the leaked and aliased RFI can be observed at the frequency F_A that depends on the F_{RFI}, the FS of observation M and the original sample rate F_m. The relationships between F_A, F_{RFI}, M and F_m are derived in the following, showing that in an FS where the RFI is non-native (i.e. $N \neq M$), F_A changes with F_m. When the imaging fine channels corresponding to two receptors associated with different F_m are cross-correlated, the difference between the aliased RFI frequencies leads to decorrelation, as per equation (1). Note that for Band 3, Mid.CBF up-samples the input sample sequences by a factor of 5/4. Hence, with respect to the input of the VCC-OSPPFB, the sample rate is $F_m = 3.96 \times 10^9 + k(A_n)\Delta F$ for Band 3.

Evaluating $F_A[F_{RFI}, M, F_m]$

Step 1: Specify the Required Parameters:

- Frequency of the RFI with respect to the baseband spectrum of the sampled sequence - F_{RFI} – in Hz.
- Frequency Slice (FS) index[a] - M.
- Actual sample rate at the receptor - F_m in Hz.
- Common sample rate of the FS - FFS_0 (= 220,200,960) in sps (samples/sec).

[a] FS index is the output channel index of the VCC-OSPPFB.

- Additional frequency shift[b] - F_{AS} in Hz.
- Number of FS produced by the VCC-OSPPFB - N_{FS}
- Over-sampling factor of the VCC-OSPPFB - OS_1 $(= 10/9)$.

Step 2: Calculating Aliased Frequency in the VCC-OSPPFB

- Actual sample rate at the output of the VCC-OSPPFB - $FFS_m = OS_1 \cdot F_m/N_{\mathrm{FS}}$ in Hz
- Direct aliased frequency of F_{RFI} – in Hz

$$FDA_m = \mathrm{mod}[F_{RFI}, FFS_m]. \tag{7}$$

- Frequency Shift aligning passband and the filtered bandwidth in the VCC-OSPPFB - in Hz

$$F\_OSPPFB_m(M, F_m) = M \cdot FFS_m \cdot (OS_1 - 1)/OS_1\ . \tag{8}$$

- Frequency of the aliased component of F_{RFI} in M^{th} FS sampled at FFS_m - in Hz

$$FA\_OSPPFB[F_{RFI}, M, F_m] = \mathrm{mod}\big[\big(FDA_m + F\_OSPPFB_m(M, F_m)\big), FFS_m\big]; \tag{9}$$

- Expressing $FA\_OSPPFB[F_{RFI}, M, F_m]$ within $[-0.5FFS_m, 0.5FFS_m]$ - in Hz

$$\begin{aligned} &\text{If } FA\_OSPPFB[F_{RFI}, M, F_m] > 0.5FFS_m; \\ &FA\_OSPPFB[F_{RFI}, M, F_m] = FFS_m - FA\_OSPPFB[F_{RFI}, M, F_m] \end{aligned} \tag{10}$$

Step 3: Calculating Aliased Frequency in the ReSampler

- Frequency shift applied to align FSs for cross-correlation - in Hz

$$ReSamp[M] = M \cdot (FFS_0 - FFS_m)/OS_1. \tag{11}$$

- The aliased frequency - in Hz

$$F_A[F_{RFI}, M, F_m] = FA\_OSPPFB[F_{RFI}, M, F_m] - ReSamp[M]\ +\ F_{AS}. \tag{12}$$

- The fine channel that the aliased frequency falls into;

$$NCH2[F_{RFI}, M, F_m] = \mathrm{mod}\left(F_A[F_{RFI}, M, F_m] \cdot \frac{N_{c2}}{FFS_0}, N_{c2}\right). \tag{13}$$

Note that the above derivation considers an RFI feature that is in the sampling bandwidth of the DSH digitizer. This may not be directly applicable for RFI that leaks through the antialiasing filter of the DSH receiver.

2.3. *Performance of the SCFO Sampling in RFI Mitigation*

As specified by SKA1_Mid Requirement 1834 (SKA1 Mid.CBF Req; Spec:), as a part of RFI mitigation, application of SCFO sampling in Mid.CBF is required to

1. achieve at least 30 dB attenuation of (aliased) RFI not native to its Frequency Slice or Search Window, in cross-correlation visibilities,

2. not limit further attenuation of such aliased RFI in cross-correlation visibilities for increased frequency offsets and/or integration times and,

3. ensure such (aliased) RFI does not add coherently in any tied-array (beamformer) outputs,

[b] Additional frequency shifts may be required to correct for the Doppler shift, and to align fine frequency channels across FSs as though all the fine channels are derived from a single channelizer.

where all three requirements are subject to fundamental limitations from DSH sample clock frequency offsets, correlator integration time, and filter Nyquist zones.

In the following, a specific scenario for Band 1 imaging processing is considered, with a strong interferer at 840 MHz carrying 30 dB power compared to the system noise. According to equation (6) this interferer falls in the 4th FS of the 20 Channel VCC-OSPPFB. However, due to the finite attenuation of the VCC-OSPPFB, some power is leaked into the other FSs. Due to the gradually increasing attenuation pattern for the stopband of the VCC-OSPPFB the leaked power is highest at the adjacent FSs. In order to evaluate the performance of SCFO sampling in the suppression of artefacts due to rotation of the Earth, the shortest baseline of 13.5 m[c] is considered, with the receptors tracking a delay-center in the zenith that is moving orthogonal to the baseline.

The simulated auto- and cross- correlations of the imaging channels corresponding to the 5th FS for two receptors A_1 and A_2 with and without SCFO sampling, which are integrated for ~0.14 s, are shown in Fig. 2. Note that the abrupt power change around channel-index 4400 corresponds to the edge of the observing band at 1.05 GHz for Band 1. The signal generator does not produce any correlating spectral components beyond this point. With SCFO sampling, the received signal at A_1 is sampled at F_1= 3.9600018 Gsps and A_2 is sampled at F_2= 3.9600216 Gsps, respectively thus corresponding to 19.8 kHz offset in the wideband. Without SCFO sampling, the received signals at both A_1 and A_2 are sampled at F_0= 3.96361728 Gsps. The auto-correlations with and without SCFO sampling show significant spectral leakage from the input tone. However, as seen in the expanded view, with SCFO sampling the leaked power in the cross-correlation is about ~16.8 dB below that in the cross-correlation without SCFO sampling.

Following equation (13), it can be calculated that with SCFO sampling the leaked spectral components fall into the 5141st and 5142nd channels with a separation of 1100 Hz, whereas without SCFO sampling they fall into the 5156th and 5157th channels in the 5th FS. In these channels, it has been observed that the uncorrelated noise power is about 9.5 dB lower than the leaked spectral components. Hence according to equation (3), the expected power at these channels is around -20.0 dB. This value agrees well with the observed -16.8 dB. The corresponding auto- and cross-correlations of the 5th FS for A_1 and A_2 integrated for ~1.4 s is shown in Fig. 3. As shown there, with the SCFO sampling the leaked power in the cross correlation continues to integrate down to -23.4 dB, whereas without it the leaked power remains the almost the same. The estimate from equation (3) is -25.0 dB.

The same simulation was conducted for the longest baseline (i.e., 160 km) where the delay is changing the fastest. In this case the residual delay and phase components associated with the leaked and aliased signal of the interferer cause decorrelation[d]. The corresponding auto- and cross-correlations for 0.14 s of integration are shown in Fig. 4, which shows the leaked power decorrelates faster with SCFO sampling. However, in this particular example, for 1.4 s of integration, where the auto- and cross correlations are shown in Fig. 5, the leaked power seems to decorrelate more with no SCFO sampling. It may be that the fringe washing effect is cancelling out the frequency shifts with SCFO sampling.

[c] That is the diameter of a dish. A MeerKAT dish is of 13.5 m diameter whereas a SKA1 dish is of 15 m diameter.

[d] Generally known as the "fringe washing" effect by astronomers.

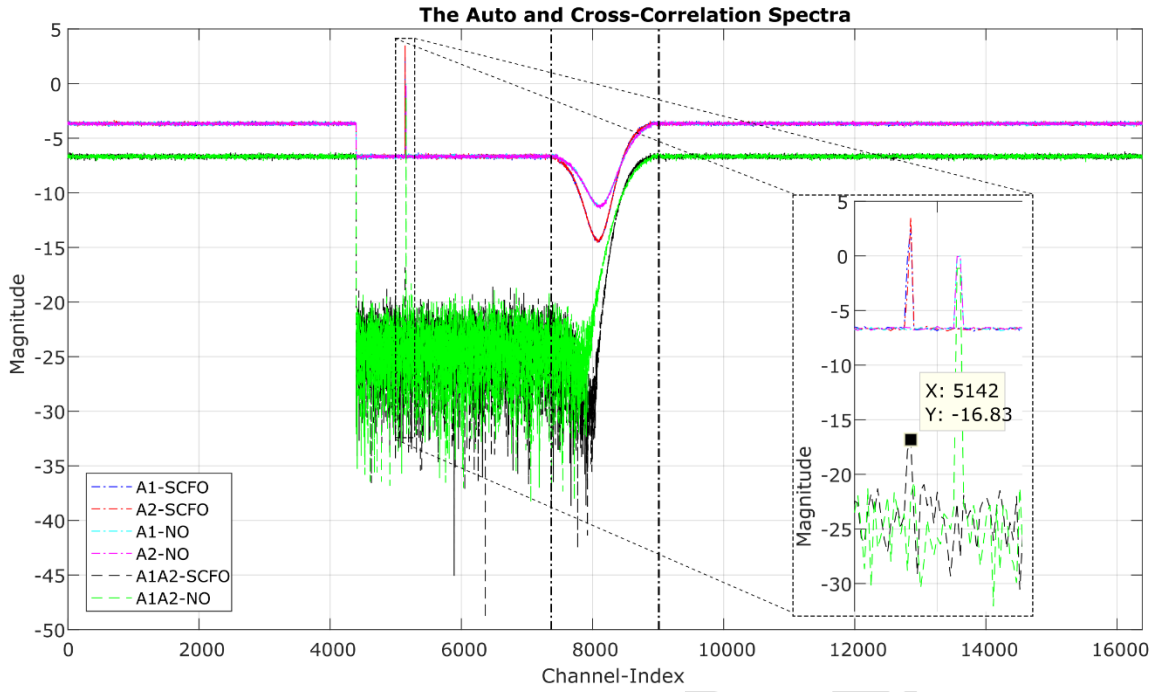

Fig. 2. Auto- and cross- correlation of imaging channels in the 5th FS integrated for ~0.14 s with and without SCFO sampling for the shortest possible baseline.

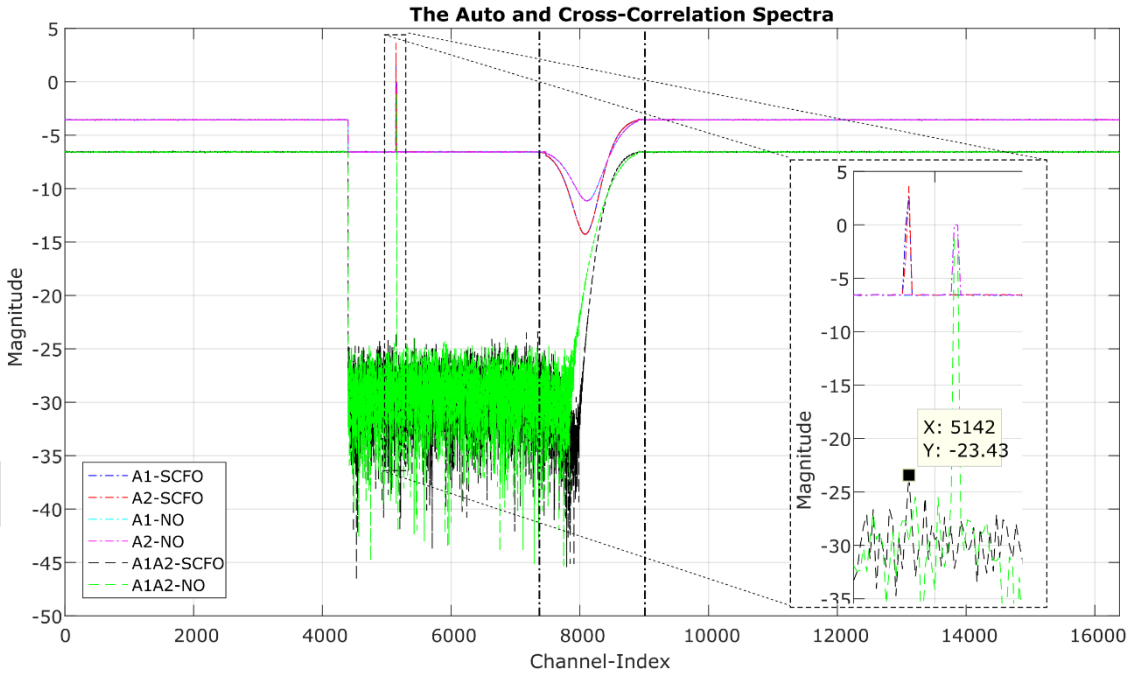

Fig. 3. Auto- and cross- correlation of imaging channels in the 5th FS integrated for ~1.4 s with and without SCFO sampling for the shortest possible baseline.

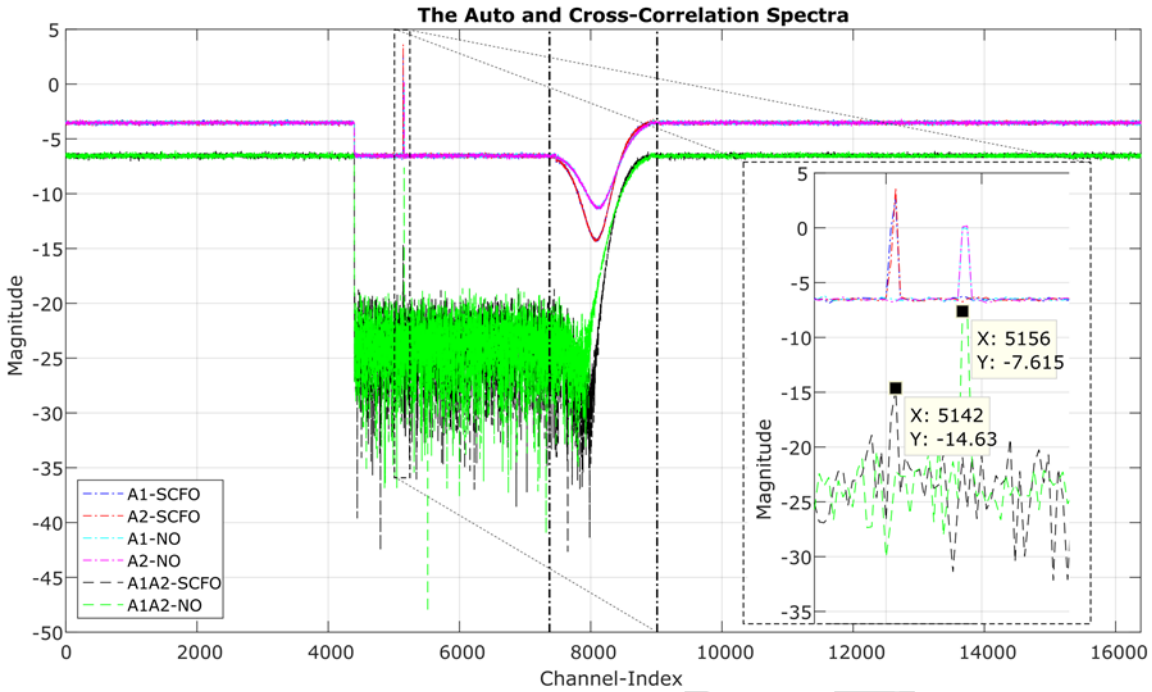

Fig. 4. Auto- and cross- correlation of imaging channels in the 5th FS integrated for ~0.14 s with and without SCFO sampling for the longest possible baseline.

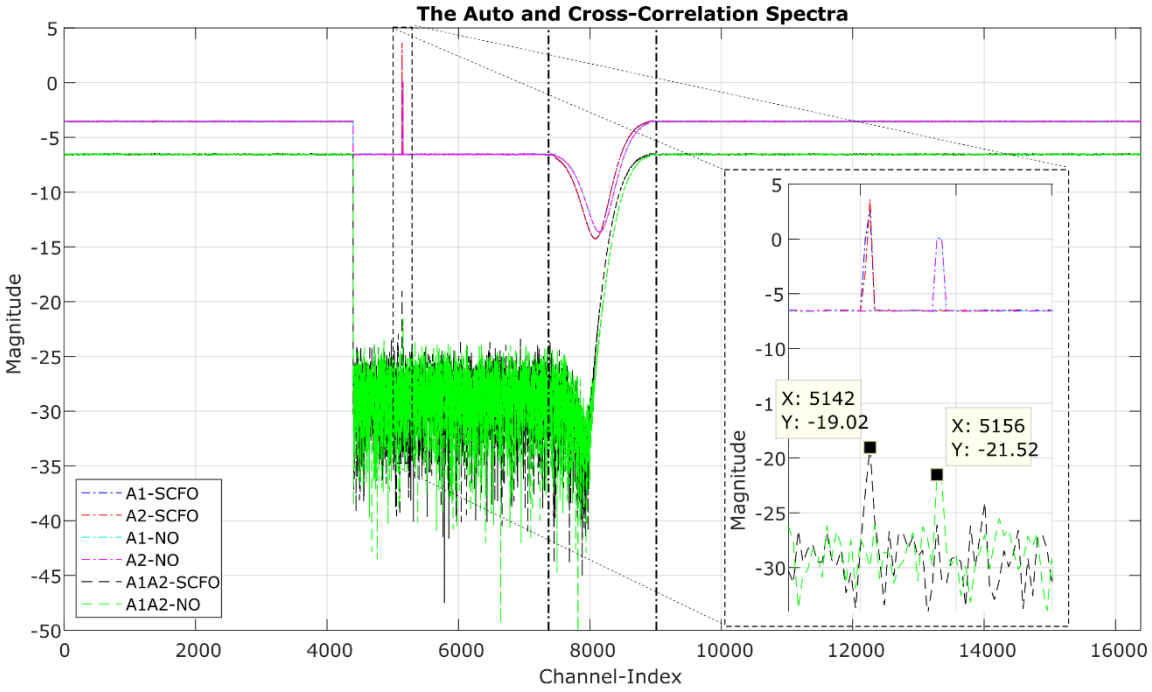

Fig. 5. Auto- and cross- correlation of imaging channels in the 5th FS integrated for ~1.4 s with and without SCFO sampling for the longest possible baseline.

3. Shift-Resample-Shift-Back Scheme to Minimize RFI Associated Noise

3.1. *The ReSamplers in the Mid.CBF*

There are several ReSamplers employed in the different signal processing paths of Mid.CBF. Here, ReSamplers are mainly used for delay, phase, and Doppler shift corrections, in addition to resampling the signal sequences sampled with SCFO sampling. Also, ReSamplers are proposed to be used to 'steer beams' in VLBI beamforming.

The basic operation of the ReSampler is illustrated in Fig. 6. Consider the continuous-time signal $x(t)$, with the points shown on $x(t)$ by blue 'O' corresponding to the original sample points. In case of delay correction, the points shown on $x(t)$ by red '\' correspond to the sample times at which $x(t)$ should have been sampled if there were no delay. In case of a change in sample rate, the points shown by red '\' correspond to the sample times for the targeted sample rate.

In (Harris, 2004), it has been proposed that a '*fractional-delay'* filter-bank, as shown in Fig. 7 (left), should be used to interpolate the sample values at the required sampling points. For the estimation of the signal value at a particular required sampling point (i.e. red '\' points in Fig. 6) a specific fractional-delay filter $H_k(z)$ is selected such that it minimizes the difference between the interpolated sample point and the required sample point. Therefore, the maximum 'ReSampler interpolation-error' between required sample point and the interpolated sample point in the resampling process is half of the delay-step achieved with the set of fractional-delay filters.

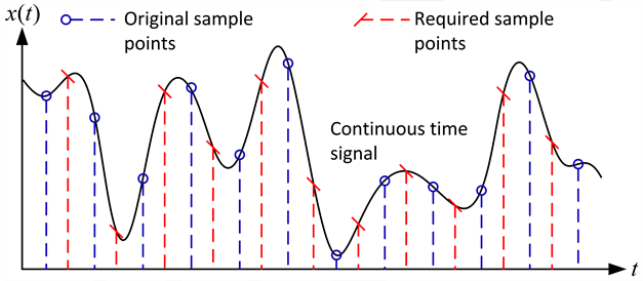

Fig. 6. The distribution of original sample points sample points and the required sample points.

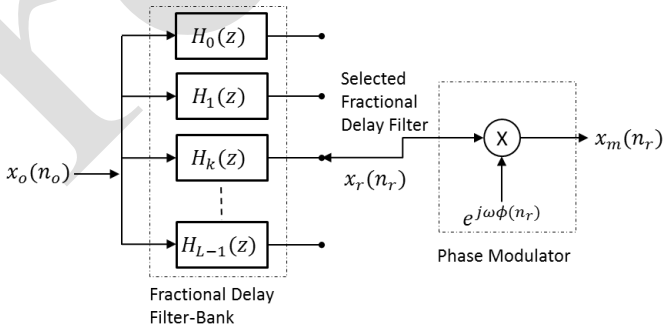

Fig. 7. A sub-optimal functional architecture for a ReSampler.

3.2. *Effects of Finite Delay Steps in the ReSampler*

Approximation of continuously varying interpolation points with fixed and finite delay steps generates interpolation errors that are a function of the rate of the delay variation. For small delay steps, the average interpolation error quickly converges to 0. However, for a sinusoid of frequency f, the delay rate translates to a periodic 'saw-tooth' shaped phase modulation varying over the range $(-\pi fDS, \pi fDS)$, where DS is the delay step of the fractional-delay filter-bank. This periodic phase modulation generates multiple replicas of the spectrum of the input signal.

Assuming linear delay variation with delay rate $\dot{\tau}$, for N-delay steps, the k^{th} harmonic of the frequencies generated by the resulting periodic phase modulation in fractional-delay filter-bank is

$$f_k = kN\dot{\tau}F_s, \tag{14}$$

where F_s is the sampling frequency. The maximum associated amplitude of the k^{th} harmonic generated for the input sinusoid of frequency f is given by

$$|A_k| = \frac{f}{kNF_s}. \tag{15}$$

This implies that even for large N (e.g., 1024) the delay rate generated harmonics can become a concern for very strong narrowband RFI (> 30 dB above the system noise level).

Experimental Study of Effects of Finite Delay Steps in the ReSampler

As described above, delay errors due to finite delay steps generate shifted copies of the input spectrum. In Mid-CBF, this is of particular interest because strong RFI is present in Bands 1, 2 and 3 (Mesa Solutions, 2018). A simulation of the ReSampler and subsequent channelizer and correlator has been carried out to empirically estimate the position and relative magnitude of the replicas of a strong tone in the input. In the following, two FSs corresponding to two receptors A_1 and A_2 are preceded by ReSamplers using a fractional delay filter-bank of 1024 delay steps and an ideal phase modulator, in order to resample those to the common sample rate of 220.20096 Msps. In the initial study, delay dithering was not enabled. The input sequences to the ReSamplers have been synthesized to represent the 5[th] FS generated from 20 channel VCC-OFPPFB for Band 1 in response to a pure tone at 945 MHz[e]. For receptor A_1, the FS sample rate is 220.0006 Msps; for receptor A_2, the FS sample rate is 220.0102 Msps. The resampled sequences are then processed by the 16k Imaging Channelizer (see Fig. 1 (b)) and correlated for 0.14 s. In Fig. 8, auto-correlation spectra for A_1 and A_2 are shown in blue and red dash-dot lines and the cross-correlation spectrum is shown in black dashed-lines. As shown there, the replicas of the tone in auto-correlations are aliased back to the spectrum and lie exactly within the channels predicted by (14). Similarly, the relative magnitudes of the replicas predicted by equation (15) agree well with the auto-correlations. However, as expected with SCFO sampling, replicas in the cross-correlation are about 100 dBs below the input signal level.

It has been observed that in ADCs, random 'clock-jitter' (i.e. dithering) reduces the amplitude of generated harmonics by spreading those across the signal spectrum at the expense of adding more noise to the signal (Texas Instruments, 2010). As stated there, the signal-to-interpolation-error noise ratio (SNR_{IE}) due to resampling of a sinusoidal input is given by

$$SNR_{IE} = -20\log(|\omega_S \tau_{IE}|) \text{ dB}, \tag{16}$$

where ω_S is the relative frequency of the sinusoid and τ_{IE} is the RMS interpolation-error in samples. If the interpolation-error is uniformly distributed within $(-0.5DS, 0.5DS)$ then $\tau_{IE} = DS/\sqrt{12}$, where DS is the delay-step. Note that the SNR_{IE} depends on the frequency of the sinusoid, such that a lower frequency sinusoid achieves a higher SNR_{IE}.

The auto- and cross-correlations achieved with a random delay dither that is uniformly distributed within $(-0.5, 0.5)$ of the delay-step in the ReSampler is show in Fig. 9. As shown there the harmonics are completely suppressed. In the scenario considered here, the expected signal-to-delay-dither noise ratio (SNR_{DD}) evaluated using equation (16) is 68.65 dB. According to (Texas Instruments, 2010), (16) and the simulation results, the excess noise generated by delay dithering depends on the relative frequency of the tone. Assuming the delay dither noise has a flat spectrum and considering the ~42.14 dB gain achieved with the 16k channelizer and ~3 dB gain in the channel

[e] At the SKA1 Mid telescope site, strong RFI is expected in the GSM band ~ 935 – 955 MHz that falls into Band 1 (Mesa Solutions, 2018).

response, the relative magnitude of the auto-correlations is expected to be -107.8 dB. This value closely matches the simulation results shown in Fig. 9.

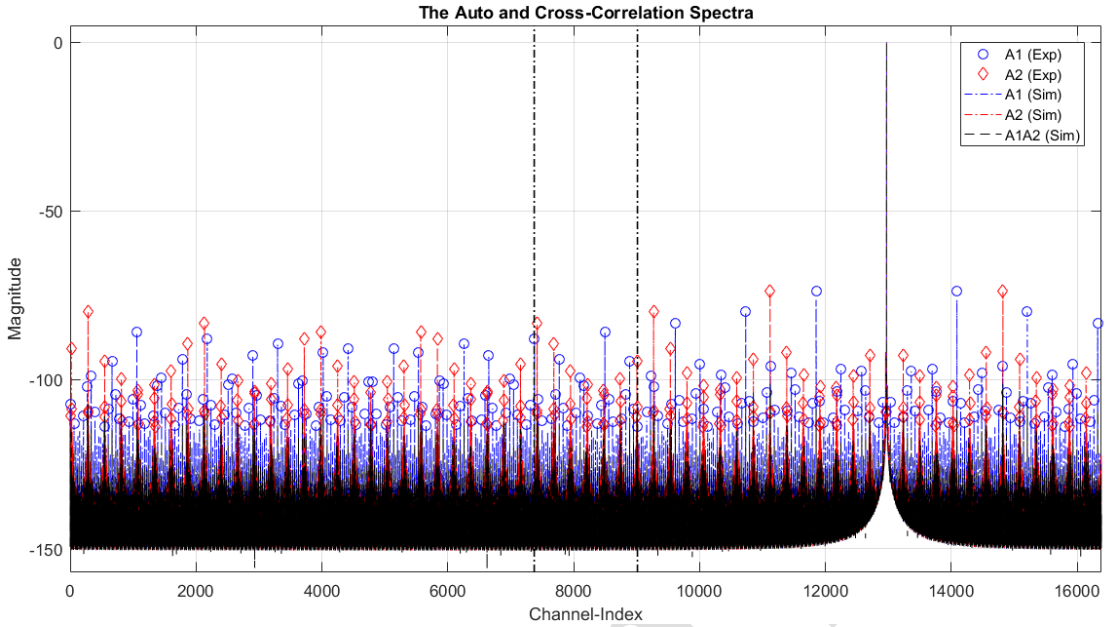

Fig. 8. Expected and simulated auto- and cross- correlations of channelized ReSampler outputs with no delay dithering.

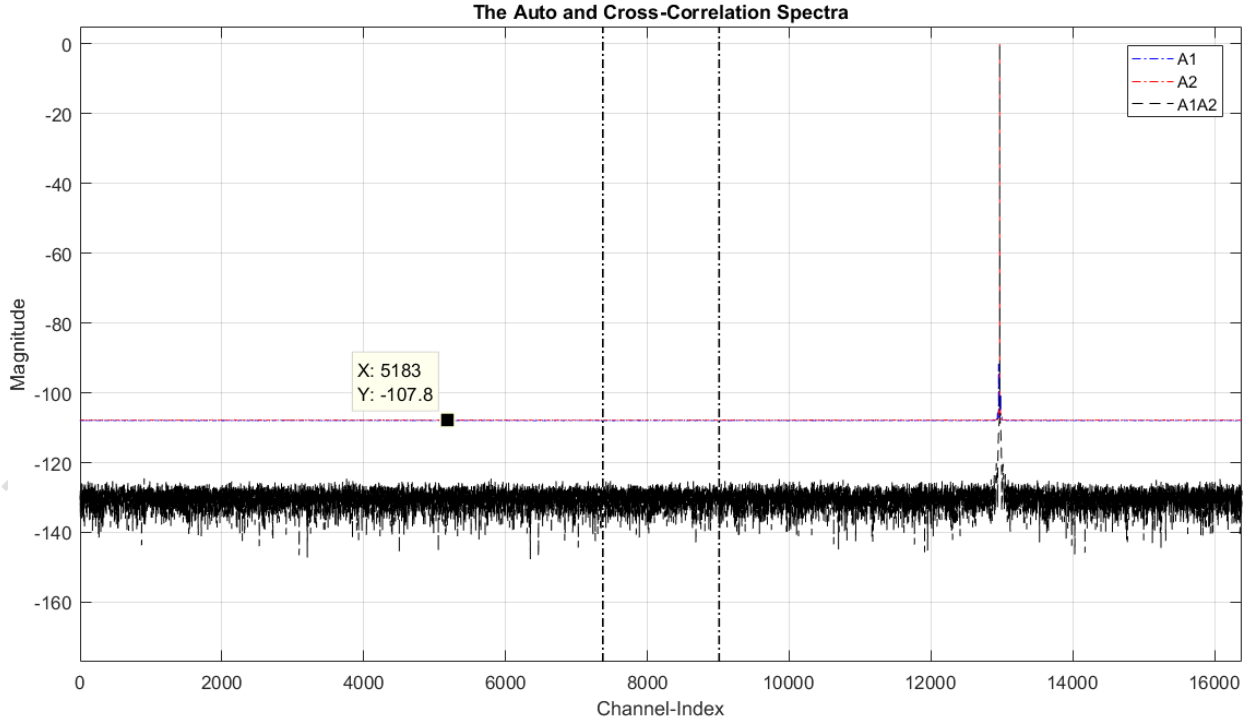

Fig. 9. Auto- and cross- correlations of channelized ReSampler outputs with delay dithering in the ReSampler.

3.3. *Effects of Finite Phase-Steps in the Phase Modulator*

Similar to the previous case, approximating a continuously varying phase with fixed and finite phase steps generates phase-errors that are a function of the rate of the phase variation. Approximating a linearly varying phase with such a Look-up-Table (LUT) as in the phase modulator of the ReSampler (see Fig. 7-right) corresponds to a true exponential multiplied by a small and fast saw-tooth function. As mentioned in the previous section, this produces a large number of harmonics in phase factor.

For the following discussion, it is assumed that the phase factors $[\cos(2\pi n/2^N); \sin(2\pi n/2^N)]$; $n \ni [0, 2^N - 1]$ are stored in a LUT. These correspond to the Cartesian coordinates of the points on the circumference of a circle with unit radius (i.e. unit-circle) at angular intervals $2\pi/2^N$ starting from the point (1, 0). Assuming linear phase variation corresponding to the constant frequency ω_0, for 2^N-phase steps in the LUT, it can be shown that the frequency of the k^{th} harmonics generated by the resulting periodic phase modulation is

$$f_k = \frac{(1 + 2^N k)\omega_0}{2\pi}, \tag{17}$$

and that the maximum of the associated amplitudes is

$$|A_k| = \frac{1}{k2^N}. \tag{18}$$

Note that with the modulator operating at discrete times, these harmonics alias into the Principal Nyquist Region. Similarly, even for large N (e.g. ,10-14) the phase-step-generated harmonics can become a concern for very strong narrowband RFI (> 30 dB above the system noise level).

Experimental Study of Effects of a Finite Number of Phase Steps in the Phase Modulator

In order to empirically evaluate the position and relative magnitude of the replicas of a strong tone generated due to such a phase error, the same input containing a single tone and the same signal processing chain used in previous section can be used with minor modifications. First, the sample rates of the input sequences to ReSamplers are selected such that there are no delay-errors (i.e. the ReSampler estimates the signal at the exact point of resampling). Here, this is achieved by selecting the FS sample rate for receptor A_1, as 219.770880 Msps and FS sample rate for receptor A_2, as 219.985920 Msps, compared to the common sample rate of 220.200960 Msps.

At the ReSampler, instead of the ideal phase rotator used in the previous case, a phase rotator based on a look-up-table (LUT) containing $2^{14} = 16{,}384$ sample points around the unit circle is used to apply a frequency shift of 7420 Hz. After subsequent channelization, the auto- and cross-correlations accumulated for a period of 0.14 s are shown in Fig. 10. The estimated positions and the relative magnitudes of the replicas of the tone are accurately predicted by equations (17) and (18).

The SCFO sampling facilitates the decorrelation of such harmonics, as samples streaming from two receptors are subjected to two different frequency shifts such that the resulting harmonics would not coincide in frequency. Also, adding some phase dithering in the phase synthesizer reduces the amplitudes generated by the harmonics. By applying a random phase dither that is uniformly distributed within $(-0.5PS, 0.5PS)$, where PS is the phase step in the phase modulator of the ReSampler the replicas in the auto- and cross-correlations can be perfectly mitigated as shown in Fig. 11. For phase dithering, in order to calculate the expected signal-to-phase-error noise ratio (SNR_{PE}), $\omega_S \tau_{IE}$ in equation (16) is replaced by the rms phase error $\frac{2\pi \cdot PS}{\sqrt{12}}$. For the example considered here $PS = 2^{-14}$ therefore, SNR_{PE} = 79.12 dB. Assuming the phase-error noise has a flat spectrum and considering the number of channels and the channel response of the channelizer, the relative magnitude of the auto-correlations is expected to be -118.2 dB. This value closely matches the simulation results shown in Fig. 11.

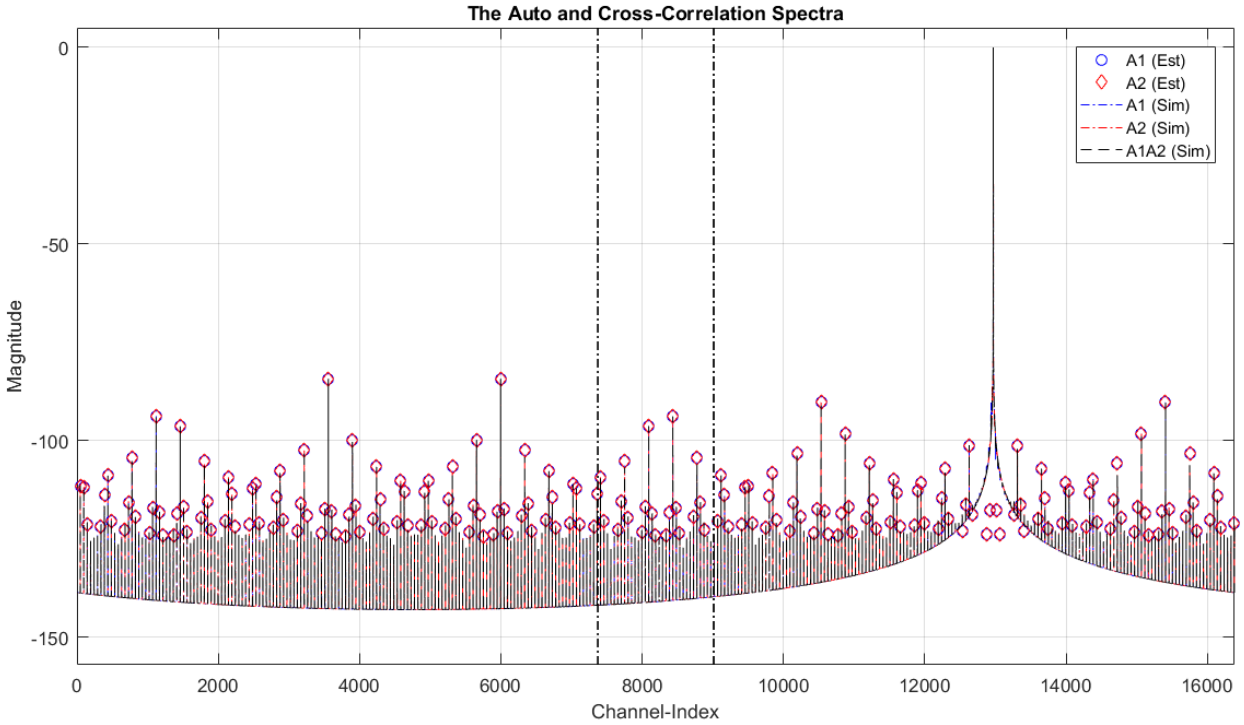

Fig. 10. Expected and simulated auto- and cross- correlations of channelized ReSampler outputs with no phase dithering.

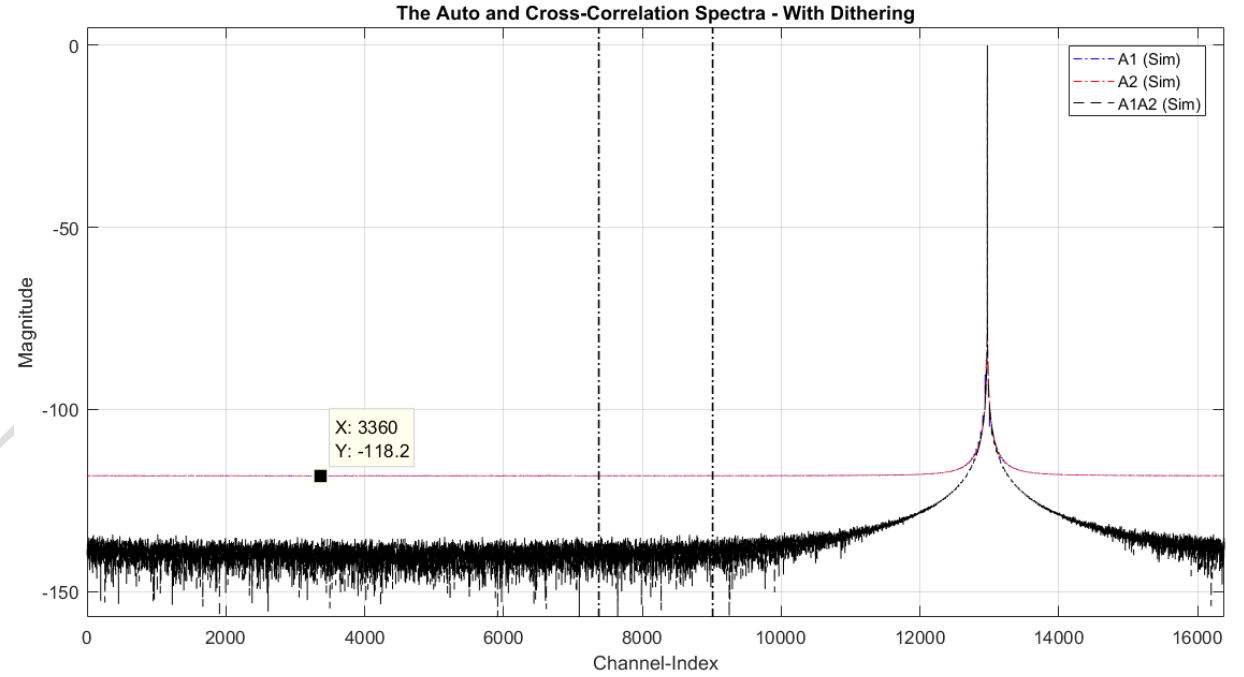

Fig. 11. Auto- and cross- correlations of channelized ReSampler outputs with phase dithering.

3.4. *Reduction of Additional Noise Generated in the Resampling due to Strong RFI*

As shown in Section 3.2, the excess noise generated by delay dithering depends on the relative frequency of the tone. According to Mesa Solutions (2018), at the SK1 Mid telescope site, strong RFI signals are clustered in ~10-20 MHz bands. For example, UHF TV broadcasting ~625 MHz, E-GSM ~885 MHz, GSM ~945 MHz and GNSS ~(1175, 1200, 1225, 1245, 1475 and 1575) MHz. Hence, shifting the FSs such that the relative frequency of the strongest RFI components are at or near 0 Hz, then processing with the ReSampler and shifting back, could significantly reduce the additional noise generated by delay dithering. The reduction of delay dithering noise decreases the noise floor and thereby increases the dynamic range of the resampled signal.

Implementation of the proposed processing requires an additional 'complex-phase modulator' before the ReSampler. The frequency shifting required to reorient the FS after the resampling can be incorporated with the other phase and frequency shifts performed in the complex-phase modulator in the ReSampler (see Fig. 7-right). Note that the original frequency shift F_{ROT} is selected such that the relative frequency (F_{ROT}/F_m) is an exact submultiple of 2^N, unless there is an additional noise contribution from the phase modulator on the order of $20 \cdot log\left(\frac{2\pi \cdot PS}{\sqrt{12}}\right)$. However, the current FPGA development environments provide relatively simple Numerically Controlled Oscillator (NCO) IP blocks that can generate phase components with a resolution of $\pi \cdot 2^{-17}$ rad or better. Hence, the additional noise contribution will be around 103.2 dB below the contaminating RFI. For RFI that clustered in a ~10 MHz bandwidth, and a ReSampler having 1024 delay steps, the proposed method can increase the worst case dynamic range from 55 dB to 95 dB.

A simulation has been conducted to empirically verify the proposed shifting scheme. First, an input containing a tone corresponding to the GSM band frequency 945 MHz is processed without the proposed shift-resample-shift-back scheme. For the simulation all phase rotators have a resolution of $\pi \cdot 2^{-17}$ rad. As shown in Fig. 9, for the channels that are not close to the tone, the auto-correlation power approaches a level of -107.8 dB. Considering the ~42.14 dB gain achieved with the 16k channelizer and ~3 dB gain in the channel response, the empirical calculation for the SNR_{DD} is 68.66 dB, which is extremely close to the theoretical estimate made using equation (16). Here, the ReSampler achieves ~10.6 effective number of bits (ENOB).

Next, the same input is processed with the proposed shift-resample-shift-back scheme. The tone at 945 MHz is contained in the 5th FS at a relative frequency of 45.904320 MHz with respect to the nominal sample rate of 220.200960 Msps. With SCFO sampling, the relative position of the tone differs from FS to FS depending on the actual sample rate. Given that strong RFI such as GSM occupies a ~10 MHz band, the FS was shifted by 50.904320 MHz, leaving a 5 MHz separation between the center of the FS and the tone. As shown in Fig. 12, for channels that are not close to the tone, the auto-correlation power approaches the level of -126.8 dB . Similarly, considering the gain of the 16k channelizer and the channel response, the empirical calculation for the SNR_{DD} is 87.66 dB, which closely agrees with the theoretical estimate of 87.91 dB made using equation (16). Here, the ReSampler achieves ~13.6 ENOB.

4. Conclusions

Recent surveys conducted in the SKA1 Mid site show that the RFI environment is challenging and it could severely impact the sensitivity and the survey speed of the telescope. Two novel methods for RFI mitigation in the SKA1 Mid.CBF have been presented. First, the pioneering SCFO sampling mitigates the leaking of RFI from one Frequency Slice to another. Depending on the frequency offset and the integration time, more than 30 dB attenuation can be achieved. Second, the 'Shift-Resample-Shift-Back' method improves the dynamic range of the ReSampler in the presence of strong and clustered RFI. With this approach, it may be possible to achieve high dynamic range imaging the spectral regions that are close to extremely strong RFI sources.

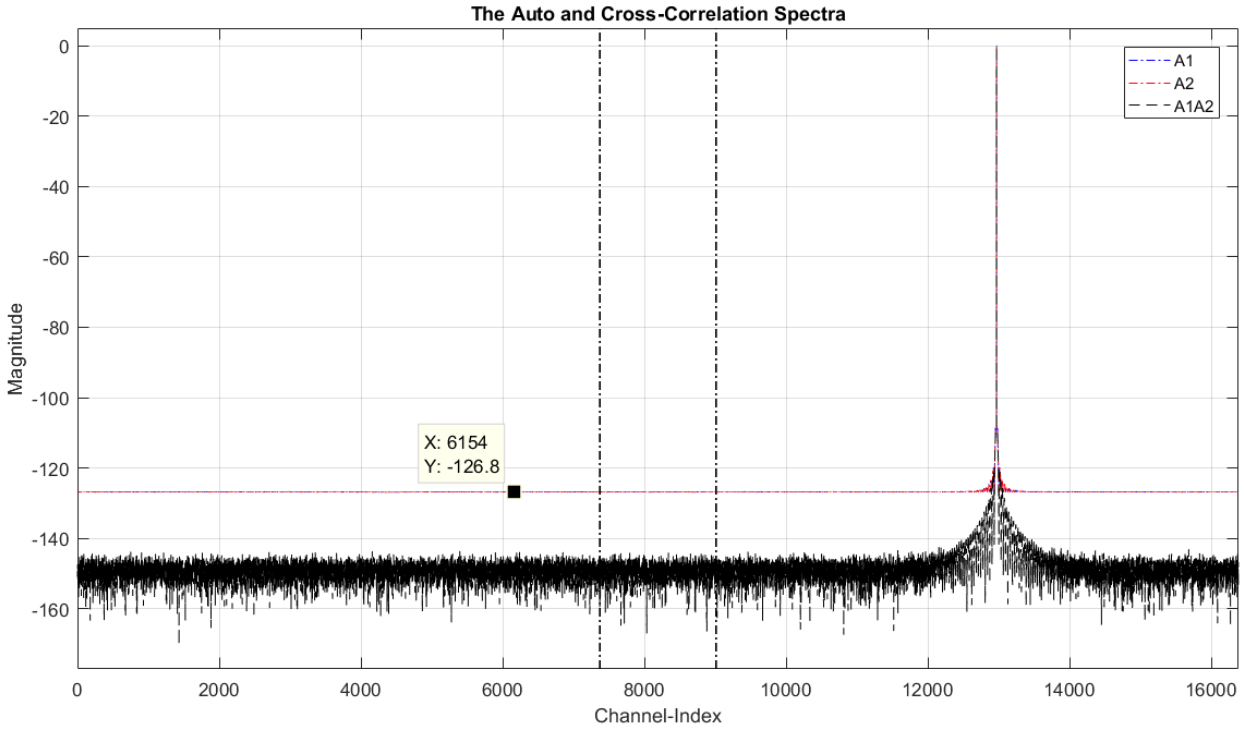

Fig. 12. Auto- and cross- correlations of channelized ReSampler outputs with shift-resample-shift-back scheme (with delay and phase dithering).

References

A Glossary of Analog-to-Digital Specifications and Performance Characteristics (Technical Report), Texas Instruments, 2010.

Astronomy Geographic Advantage Act, 2007 (No. 21 of 2007), Republic of South Africa.

National Radio Frequency Plan 2013 (NRFP-13) 8kHz to 3 GHz - Independent Communications Authority of South Africa 2013, Government Gazette, Republic of South Africa, No. 36336, Vol. 576, June 2013 Part 1 of 2.

On-Site Wideband Spectrum Measurements (Technical Report), Mesa Solutions (Pty) Lt. 2018 March 05.

SKA1 CSP Mid Correlator and Beamformer Sub-element Requirement Specification (EB-1) 311-000000-006 (Rev. 2).

Carlson B., Sample Clock Frequency Offset (SCFO) Resolution Team 3 investigation, SKA-CSP Memo-0021, 2016-03-21.

Carlson B., Gunaratne T., Signal processing aspects of the sample clock frequency offset scheme for the SKA1 Mid telescope array, 32nd URSI GASS, Montreal, 19-26 August 2017.

Dewdney P, RFI Characterisation and SKA1 Signal Chain Design Considerations,

Gunaratne T, Rupen M, and Carlson B, RFI Detection and Flagging in the SKA1-Mid Correlator Beamformer, RFI20106, Socorro, New Mexico, 17-20 October 2016.

Harris F.J., *Multirate Signal Processing for Communication Systems*, Prentice Hall, Upper Saddle River, N.J., 2004.

Woyczynski W., *A First Course in Statistics for Signal Analysis*, Birkhäuser, 2nd Ed, New York, 2010.